



TECHNICAL UNIVERSITY OF CLUJ-NAPOCA

ACTA TECHNICA NAPOCENSIS

Series: Applied Mathematics, Mechanics, and Engineering

Vol. 66. Issue Special II. October. 2023

TRANSPORT PROPERTIES OF CERIUM OXIDE DOPED IN GADOLINIUM USED FOR ELECTRICAL BATTERIES MANUFACTURE

Diana-Irinel BĂILĂ, Sergiu TONOIU

Abstract: *In engineering practice, solid electrolyte fuel cells are an increasingly considered alternative for the generation of clean energy, but the high operating temperatures required (800°C - 1000°C) can be an obstacle to commercialization. So, there is research on materials that can be used at lower temperatures. To reduce potential losses, it is necessary to find an electrolyte having good ionic conductivity and low electronic conductivity. Doped cerium oxide is strongly considered as a replacement for yttrium oxide stabilized zirconium oxide, that it is used frequently. It is important to know its electrical properties before using it in a commercial automotive battery. Different compositions of doped cerium oxide have been studied: 10% and 20% doping with gadolinium. Cerium oxide can be doped with different materials, such as: samarium and gadolinium as well as lanthanum and yttrium. This oxide presents, at low temperatures, a higher conductivity than zirconia ($ZrO_2 - 10 \text{ mols } \% Y_2O_3$), which permits the operating temperature of electrochemical batteries to lower. In this paper the elaboration of polycrystals of cerium oxides doped in gadolinium and their electrical characterization were presented.*

Key words: *Cerium oxide, SEM analysis, EDAX analysis, Gadolinium, electrical conductivity.*

1. INTRODUCTION

In literature, due to the great soot oxidation activity of CeO_2 -containing metal oxides, the catalysts with ceria-based presented a huge interest concerning the research of soot oxidation. The oxidation states enable cerium oxides to release and store atomic oxygen, permitting the easy redox transfer of the Ce^{3+} and Ce^{4+} [1-8].

Some rare earth elements (such as La, Pr, and Sm) and zirconium have been used as dopant into the ceria framework to great OSC (oxygen storage capacity) and redox properties, and to confer high-temperature stability. Some elements supported on ceria, such as K/ceria, Co/ceria, Ba,K/ceria, Cu-V/ceria, Ag/ceria, and Cu/ceria have also been researched by Yuan X et al. [2].

Nanoporous mesoporous cerium oxide with hard template has a special combination of thermal stability, large area of surface and short diffusion lengths concerning the mass and gas transport, making it interesting for high temperature catalysis, detection, and electrochemical applications, considered Baiutti F et al. [1].

Nanocrystalline materials with 10 – 100 nm are a new type of materials, having a unique potentially and until now presenting unknown physical/chemistry properties.

During the decreasing grain size of particles, the contribution of interfacial components grows a lot. Findings to date include metal-like behavior of ceramic (superplasticity), improved catalytic behavior, ceramic-like behavior of metals, and respectively the superparamagnetic of ferromagnetic materials, all in the nanocrystalline state, considered Chiang Y [4]. Electrical conductivity and thermoelectric power are established on a single crystal of $Gd_{3.0}Sc_{1.8}Ga_{3.2}O_{12}$ (GSGG) between 1273 and 1673 K.

The measurements are realized both in air and in different controlled atmospheres, and P_{O_2} being between from $10^{-1.68}$ to $10^{-5.6}$ MPa.

The data showed GSGG may well be a mixed conductor at this temperature and P_{O_2} range, having n -type electronic conductivity and ionic transport on the oxygen sublattice. Variation of temperatures induce long-lived disequilibrium in the electrical conductivity of GSGG (over 30

h at $T < 1373$ K), because the cation distribution depends in function of temperature.

The effective activation energy for equilibrium electrical conductivity is $E_a = 2.40 \pm 0.05$ eV, as opposed to values of $E_a = 1.8 - 2.2$ eV during actual temperature variation.

A greater contribution in the equilibrium E_a , grace to thermally activated cation redistribution, can explain for the higher value seen, remarked Schwartz K.B. et al. [7].

Chiang Y.M. studied different simultaneous conductivities and thermopower measurements realized on partially sintered nanocrystalline cerium oxide (~ 15nm grain size) over 10^{-3} to 1 atm of oxygen pressure varying with the temperature (between 450°C - 550°C) [4].

Mixed conduction was apparent in the oxygen pressure dependence of conductivity, although electronic conduction predominates.

Electronic mobility was performed with a small polaron hopping energy like that of bulk cerium oxide (~0.5 eV).

The oxygen vacancy migration energy was ~ 1.6 eV, much larger than in bulk ceria, but not in consistent with grain boundary values or bulk values at low temperatures (grace vacancy-dopant association).

For nanoceria, the reduction enthalpy was 1.84 eV, less than half of the corresponding result in bulk ceria.

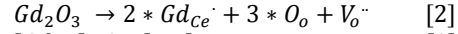
The undoped nanoceria has much larger defect populations (vacancies, electrons) and electron populations for doped nanoceria (i.e., trivalent cations), but these results are discussed in terms of the role played by the high surface, the grain boundary and the transport properties of nanocrystalline oxides [1-8].

2. ELECTRICAL CONDUCTIVITY OF DOPED CERIUM OXIDE

The specific defects for ceria CeO_{2-x} are at the origin of the stoichiometry order (x). Their concentration can be important, due to the mixed valence effects of the cation (Ce^{3+} , Ce^{4+}). The parameter x characterizes the set of atomic defaults present on the sublattice of majority defaults, as in the equation 1.

$$[V\ddot{o}] = c * K(T)^{\frac{1}{3}} * P_{O_2}^{-\frac{1}{6}} = c * P_{O_2}^{-\frac{1}{6}} * \exp\left[-\frac{\Delta H_f}{3R*T}\right] \quad [1]$$

Where: ΔH_f - enthalpy of formation for one mole of defect points, c - constant, R- universal gas constant (= 8.314 J*K⁻¹*mol⁻¹), T - temperature (K), P_{O_2} - partial pressure of oxygen in the gaseous phase in equilibrium, $V\ddot{o}$ - vacancies, that are predominant defects if $x < 1$. When the oxide is doped with gadolinium, the concentration of point defects is essentially controlled by the dopant, as in the next equations 2 and 3:



$$[Gd_{Ce}] \sim 2 * [V_o^{\ddot{o}}] \quad [3]$$

So it is possible therefore to consider, as a first approximation, that the concentration of oxygen vacancies is independent of P_{O_2} .

The law of variation of electrical conductivity with the temperature, at constant oxygen pressure can be written, such in formula 4:

$$\left[\frac{\partial \log \sigma}{\partial (1/T)}\right]_{P_{O_2}} = -\frac{\Delta H \sigma}{2.3} * R \quad [4]$$

where $\Delta H \sigma$ is the mobility activation energy of point defects.

In the case of cerium oxide doped with gadolinium, the electrical conductivity can be considered independent of the partial pressure of oxygen in equilibrium with the oxide (eq. 3). In these conditions, as in 5 and 6:

$$\left[\frac{\partial \log \sigma}{\partial \log P_{O_2}}\right]_T \sim 0 \quad [5]$$

$$\left[\frac{\partial \log \sigma}{\partial (1/T)}\right] = \Delta H \mu \quad [6]$$

where $\Delta H \mu$ is the mobility activation energy of point defects $[V_o^{\ddot{o}}]$.

To determine the electrical conductivity, a solid electrolytic cell is used, and the e.m.f. measured at the probe terminals depends on the partial pressure of oxygen in the gaseous phase, as in equation 7:

$$E = E^{II} - E^I = \frac{R * T}{4 * F} * \ln \frac{P_{O_2}^{II}}{P_{O_2}^I} \quad [7]$$

Where $P_{O_2}^{II}$ represents the partial pressure of oxygen in equilibrium with the oxide and $P_{O_2}^I$ represents the reference partial pressure of oxygen (air/0.21 atm). This electromotive force E is measured using a Tacussel millivoltmeter (type Aries 20000), having an input impedance $> 10^{12}$ ohm.

3. COMPLEX IMPEDANCE SPECTROSCOPY

The measurements were carried out by complex impedance spectrometry (C.I.S.) using a Schlumberger impedance meter (1260 series), in

the frequency range 10^{-2} - $2 \cdot 10^7$ Hz. The electrical conductivity measurements were carried out for five samples cold isostatically compacted (4000 bar), then sintered (samples B, C, D, F and G) and for a sample sintered by hot uniaxial pressing (sample P2), as in the table 1.

Table 1
Sintering conditions of CeO₂ pure and doped in Gd

Characteristics	Sintering	Sample	d	Φgrains
CeO ₂ micronized	1600C/15h/air	A	99 %	30-50 μm
CeO ₂ opaline	1600C/30h/air	E	96 %	10 μm
CeO ₂ HAS doped	1650C/15h/Argon C	B	96 %	5-7 μm
CeO ₂ HAS doped	1600C/15h/air	C	81 %	7-10 μm
CeO ₂ HAS doped	1600C/15h/air	D	82 %	5-7 μm
CeO ₂ HAS doped	1650C/30h/air	F	78 %	14-17 μm
CeO ₂ HAS doped	1650C/30h/air	G	77 %	7-10 μm
CeO ₂ HAS doped	1300C/1h/uniaxial pressure 25 MPa	P2	95 %	1 μm
CeO ₂ opaline micronized	1300C/1h/uniaxial pressure 25 MPa	P4	94 %	0.5-1 μm

The electrical conductivity measurements were realized in air, in function of the temperature variation between 200°C-700°C, after verifying that the results were not influenced by PO₂.

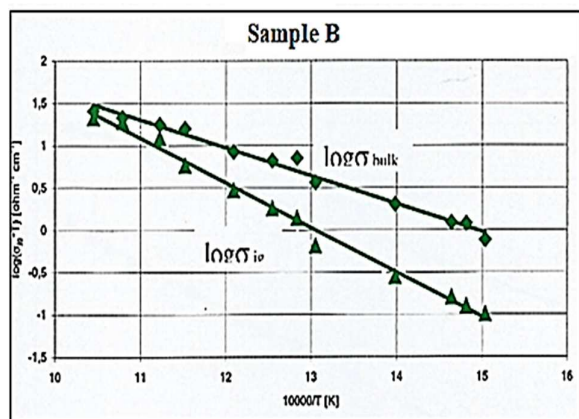


Fig.1. Electrical conductivities varying with the inverse of the temperature for the sample B

In Figures 1-6, they are presented the electrical conductivities $\log \sigma_{\text{bulk}}$ and $\log \sigma_{\text{jg}}$ obtained varying with the inverse of the temperature for the samples B, C, D, F, G and P2.

It can be noticed that the values of the conductivity of the grains are the same for the different samples.

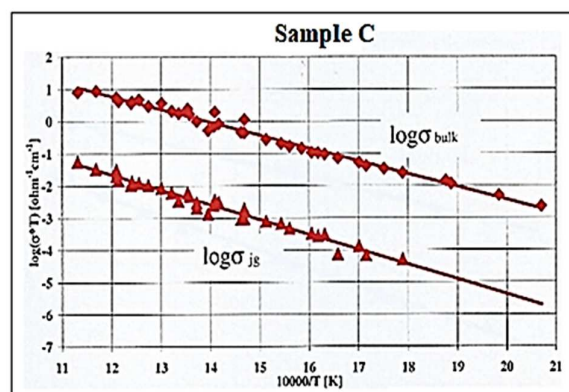


Fig.2. Electrical conductivities obtained varying with the inverse of the temperature for the sample C

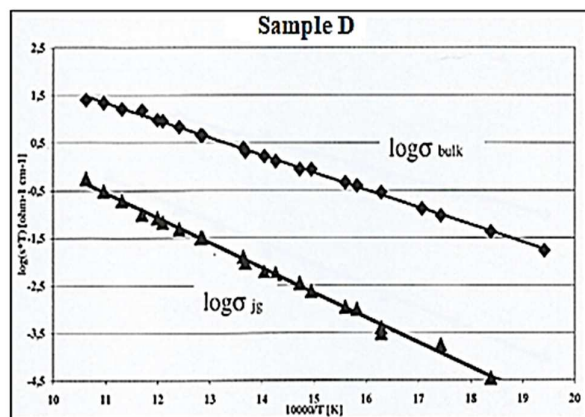


Fig.3. Electrical conductivities varying with the inverse of the temperature for the sample D

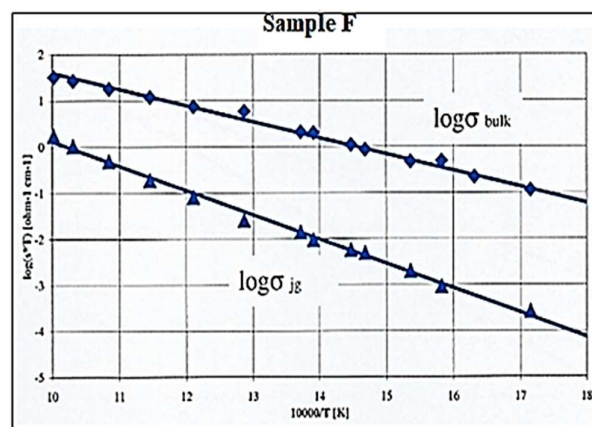


Fig.4. Electrical conductivities varying with the inverse of the temperature for the sample F

The sample P2 presents very high electrical conductivity due to the finer granulometry. It is the same for the results concerning energy activation ($E_a=0.068\text{eV}$).

The conductivity of the grain boundaries is higher for the samples having a density close to 95%, but the energy activation is not influenced by the sintering conditions ($E_a=0.104\text{eV}$).

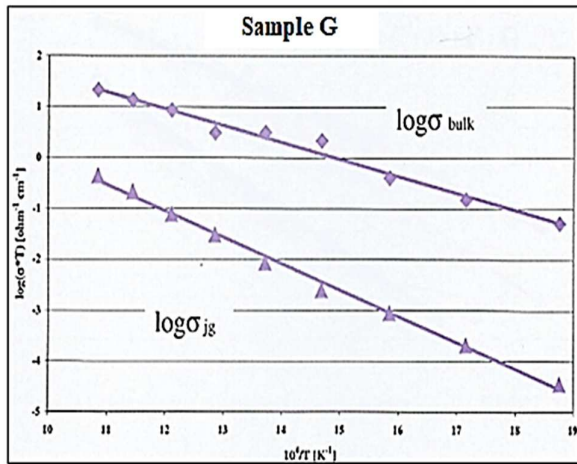


Fig.5. Electrical conductivities varying with the inverse of the temperature for the sample G

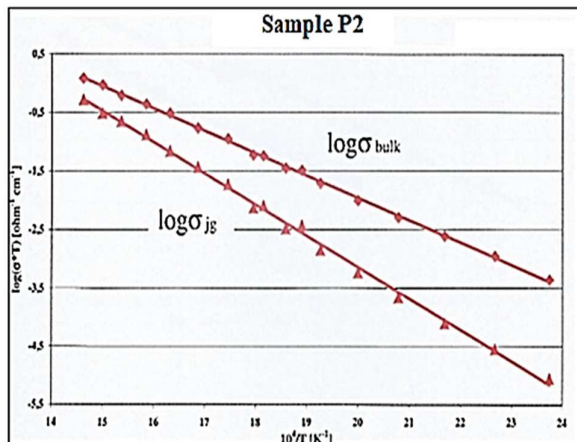


Fig.6. Electrical conductivities varying with the inverse of the temperature for the sample P2

In figures 7, 8 and 9, SEM and EDX analysis of ceria doped with Gd are presented in different conditions and can remark that the thermic treatment realized in argon C, after the sintering process, conducted to a better densification of the structure. The morphology and semi-quantitative analysis of sintered disks were investigated by scanning electron microscope QUANTA INSPECT F equipped with electron

gun with field emission -FEG (field emission gun) with a resolution of 1.2 nm and X-ray spectrometer for energy dispersion (EDS) with a resolution of 133 eV at MnK.

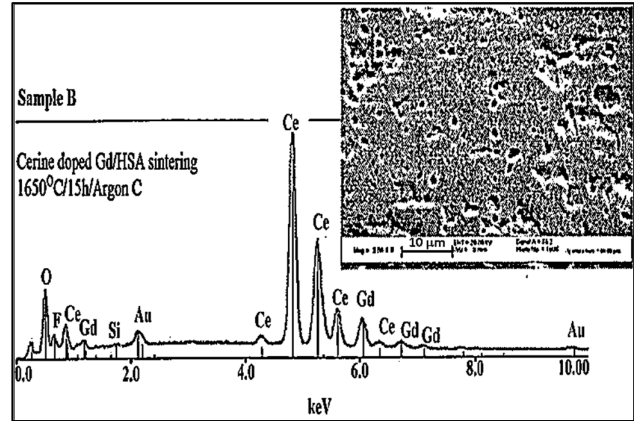


Fig.7. SEM and EDX analysis of ceria doped Gd/HSA sintering at 1650°C/15h/Argon C

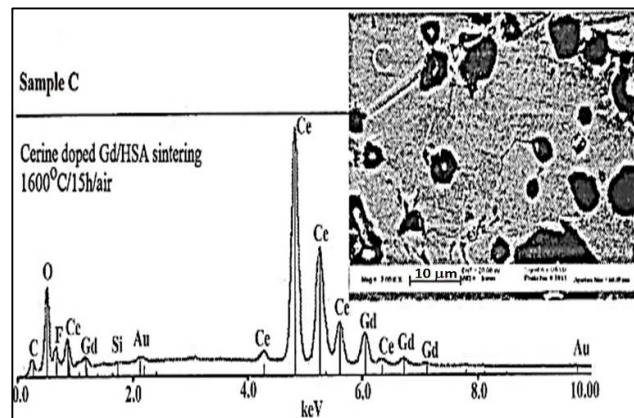


Fig.8. SEM and EDX analysis of ceria doped Gd/HSA sintering at 1600°C/15h/air

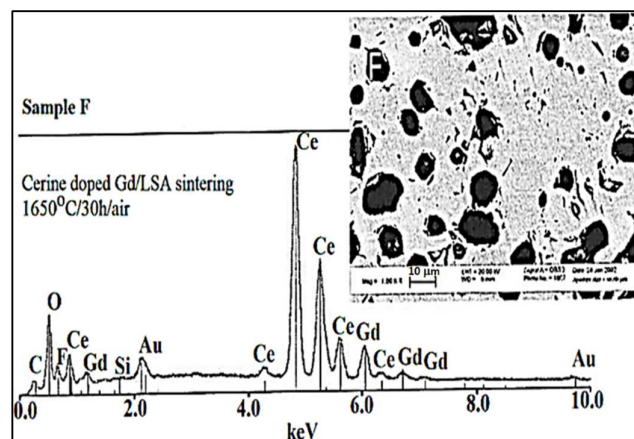


Fig.9. SEM and EDX analysis of ceria doped Gd/LSA sintering at 1650°C/30h/air

Table 2

Conductivity measurements in isotherm condition for the sample P4 (ceria opaline micronized)

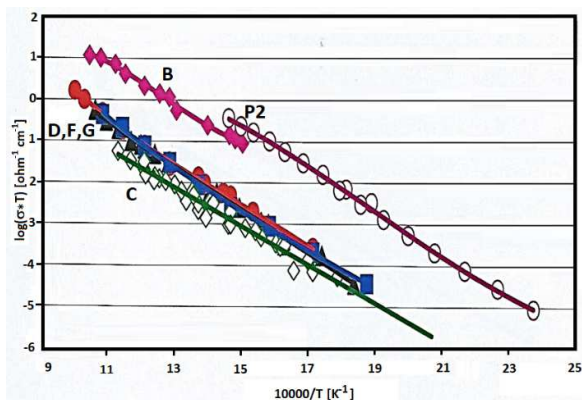


Fig.10. Results of total electrical conductivity obtained on samples B, C, D, F, G, P2

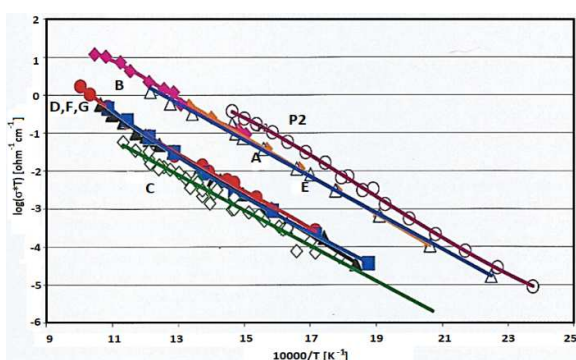


Fig.11. Results of total electrical conductivity obtained on Ceria doped samples and the literature results

The results of total electrical conductivity obtained on samples B, C, D, F, G, P2 of ceria doped in Gd are presented in figure 10 and can remark that the sample P2 presents better electrical conductivity. In figure 11 is presented the comparison between our results obtained for the samples doped in Gd with the literature results (of Tuller) and remark that the samples of ceria doped in Gd presents better transport properties that the sample of ceria presented in literature results.

In the case of ionic conductors, the complex impedance spectroscopy (C.I.S.) is made up of a succession of circular arcs which reveal that different phenomena occur in the measurement cell, with their own time constants.

In table 2, are presented the conductivity measurements in isothermal condition for sample P4 (ceria doped in Gd).

For $T < 1100^{\circ}\text{C}$ et $P_{\text{O}_2} > 10^{-7}$ atm, the electrical conductivity values are superior to sample A, being influenced predominantly by grain boundaries at low temperature.

T=900°C, geometrical factor g=8.5171 – P4

E [mV]	R [Ohm]	Log(PO2)	Log(s)
-0.6	301.3	-0.68	-1.54
-81.7	273.1	-2.08	-1.5
-53.4	284.6	-1.59	-1.52
-35	290.4	-1.28	-1.53
-70.3	277	-1.88	-1.51
-39.1	310.5	-0.01	-1.56
-153	293	-3.31	-1.53
-157	292.5	-3.37	-1.53
-159.6	292	-3.42	-1.53
-97.1	295.7	-2.34	-1.54
-184.4	288.2	-3.85	-1.53
-212.2	282.1	-4.32	-1.52
-223.5	278.3	-4.52	-1.51
-643.3	60.2	-11.74	-0.84
-229.1	262.2	-4.61	-1.48
-425.1	169.1	-7.99	-1.29
-472.8	136.2	-8.81	-1.2

T=1000°C, geometrical factor g=8.5171

E [mV]	R [Ohm]	Log(PO2)	Log(s)
-630.3	16.9	-10.67	-0.29
-696.6	9.8	-11.72	-0.06
-746.6	7.2	-12.51	0.07
-731.5	7.4	-12.27	0.06
-739.4	7.68	-12.4	0.04
-739.6	7.77	-12.4	0.03
-747.7	7.57	-12.53	0.05
-836.3	5.3	-13.93	0.2
-0	261.3	-0.67	-1.48
39.6	278.6	-0.04	-1.51
-730.4	7.97	-12.25	0.02

T=1100°C, geometrical factor g=8.5171

-963.5	2	-14.84	0.62
-1003	1.8	-15.42	0.67
-1058	2	-16.23	0.62
0	229.6	-0.67	-1.43
43.4	270.1	-0.03	-1.5
37.2	262.8	-0.13	-1.48
25.7	525.1	-0.29	-1.47
20.7	248.6	-0.37	-1.46
3.9	231.5	-0.62	-1.43
-599.8	7.29	-9.49	0.06
-347.9	38	-5.79	-0.64
-611.9	6.86	-9.67	0.09
-644.7	5.1	-10.15	0.22
-228.1	63.4	-4.03	-0.87
-340	35.3	-5.67	-0.61
-617.9	6.2	-9.76	0.13
-705.2	3.65	-11.04	0.36
-827.5	2.3	-12.84	0.56
-69.8	161.4	-1.7	-1.27

T=1200°C, geometrical factor g=8.5171			
-76.4	75.2	-1.72	-0.94
-76.3	74	-1.72	-0.93
-111.5	63	-2.2	-0.86
-476.1	8.24	-7.2	0.01
-577	4.7	-8.58	0.25
0	100.7	-0.67	-1.07
46.9	120.1	-0.03	-1.14
T=1300°C, geometrical factor g=8.5171			
49.6	54	-0.04	-0.8
-0.8	42.3	-0.68	-0.69
-87.6	28.7	-1.8	-0.52
-201	14.9	-3.25	-0.24
-494.4	3	-6.98	0.45
-417.4	4.92	-6.03	0.23
-536.1	2.33	-7.55	0.56
-683.5	1.4	-9.44	0.78
-831.9	1.32	-11.35	0.8

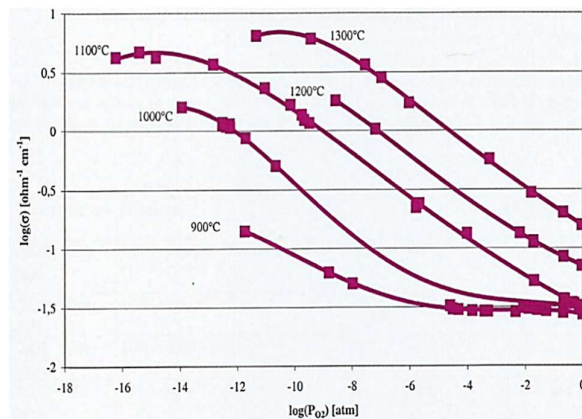


Fig.12. Electrical conductivity varying with the partial pressure of oxygen, for temperature between 700°C and 1400°C, for the sample P4 (ceria doped in Gd)

Electrical conductivity varying with the partial pressure of oxygen, for temperature between 700°C and 1400°C, for the sample D (ceria doped in Gd) is shown in figure 12, it can remark an improvement of electrical conductivity for the sample P4 in rapport with sample A.

Table 3

Conductivity measurements in isothermal condition for sample A (ceria non-doped)

T=700°C, geometrical factor g=3.1 – Sample A			
E [mV]	R [Ohm]	Log(PO2)	Log(s)
-106	910	-2.95	-2.46
-478	404	-10.59	-2.11
28.9	1240	-0.07	-2.6
10	1200	-0.47	-2.58
-13.5	1123	-0.95	-2.55
-23	1081	-1.15	-2.54
-34.4	1040	-1.39	-2.52
-478	404	-10.59	-2.11
T=800°C, geometrical factor g=3.1			

E [mV]	R [Ohm]	Log(PO2)	Log(s)
0	580	-0.67	-2.27
0	586	-0.67	-2.27
-181	380	-4.08	-2.08
-776	27	-15.27	-0.94
-660	63	-13.09	-1.3
-648.6	82.3	-12.87	-1.42
-283.3	269.5	-6	-1.93
-469.4	183	-9.5	-1.77
-492.6	163.43	-9.94	-1.72
-492.6	163.43	-9.94	-1.72
T=900°C, geometrical factor g=3.1			
E [mV]	R [Ohm]	Log(PO2)	Log(s)
0	285.1	-0.67	-1.96
0	302	-0.67	-1.98
-197	182	-4.06	-1.76
-34	334.7	-1.26	-2.03
-37.1	271	-1.31	-1.94
-62.9	248.7	-1.76	-1.9
-402.6	84.3	-7.6	-1.43
-750.6	7.9	-13.59	-0.4
-652.4	14.9	-11.9	-0.68
-520.2	40.79	-9.62	-1.11
-652.4	14.91	-11.9	-0.68
-750.6	7.9	-13.59	-0.4
-402.6	84.3	-7.6	-1.43
T=1000°C, geometrical factor g=3.1			
0	176	-0.67	-1.75
39.6	200	-0.04	-1.81
-16.6	174	-0.94	-1.74
-4.1	203.2	-1.32	-1.81
0	183	-0.67	-1.77
-653.1	5.06	-11.03	-0.21
-602.6	7.85	-10.23	-0.4
-451.9	20.57	-7.84	-0.82
-804.2	1.57	-13.42	0.29
-232.6	66	-4.36	-1.32
-256.2	53	-4.73	+1.23
-70.9	120	-1.8	-1.58
-185.6	82	-3.62	-1.42
-34.4	147	-1.22	-1.67
-44.6	142	-1.38	-1.66
-96.3	120	-2.2	-1.58
-146	96.56	-2.99	-1.49
-230.1	64.7	-4.32	-1.31
-185.66	82.3	-3.62	-1.42
-70.9	120	-1.8	-1.58
-804	1.57	-13.42	0.29
-451.9	20.57	-7.84	-0.82
-653.1	5.06	-11.03	-0.21
-602.6	7.85	-10.23	-0.4
T=1100°C, geometrical factor g=3.1			
0	92	-0.67	-1.47
0	94	-0.67	-1.48
-24.7	104	-1.04	-1.52
-6.4	97.5	-0.77	-1.49
-19.9	87.8	-0.97	-1.45
-52.2	76.5	-1.44	-1.39

T=1100°C, geometrical factor g=3.1			
-164	45.1	-3.08	-1.16
-732	1.17	-11.44	0.42
-661	1.72	-10.4	0.25
631.9	2.04	-9.96	0.18
-526.5	3.74	-8.41	-0.08
-410	8.68	-6.7	-0.44
-306.6	16.68	-5.18	-0.73
-251.6	23.06	-4.37	-0.87
45.5	112	-0.01	-1.55
T=1200°C, geometrical factor g=3.1			
0	40.3	-0.67	-1.11
48.6	50.4	-0.01	-1.21
11.5	42.69	-0.52	-1.13
-24	36.1	-1	-1.06
-62.7	29.7	-1.53	-0.98
-102	24.32	-2.07	-0.89
-89.8	25.28	-1.9	-0.91
-199	14.06	-3.4	-0.65
-220	12.35	-3.69	-0.6
-232	11.3	-3.85	-0.56
-433	3.6	-6.61	-0.06
-746	0.72	-10.89	0.63
-740	0.74	-10.81	0.62
-639	1.12	-9.43	0.44
-513	2.24	-7.7	0.14
T=1300°C, geometrical factor g=3.1			
0	16.44	-0.67	-0.72
-15.6	15.39	-0.87	-0.69
52.6	21.61	-0.01	-0.84
-807	0.55	-11	0.74
-783.6	0.56	-10.73	0.74
-779	0.57	-10.67	0.74
-737.4	0.6	-10.13	0.73
-684	0.54	-9.45	0.7
-641.5	0.8	-8.9	0.68
-583.2	1.85	-8.16	0.58
-421.9	5.46	-6.09	0.22
-208	5.48	-3.34	-0.24
T=1400°C, geometrical factor g=3.1			
0	7.28	-0.67	-0.37
-606.3	0.56	-7.99	0.74
-515.5	0.7	-6.84	0.64
-413	0.96	-5.66	0.5
-331	1.6	-4.67	0.28
-329.4	1.68	-4.65	0.26
-164.8	3.21	-2.66	-0.01
-157.7	3.45	-2.58	-0.04
-85.1	4.76	-1.7	-0.18
-44	5.84	-1.2	-0.27
55	9.43	-0.01	-0.48

In table 3, are presented the conductivity measurements in isothermal condition for sample A (ceria non-doped). For $T > 1200^\circ\text{C}$ and $P_{\text{O}_2} > 10^{-8}$ atm, $\log \sigma$ varies linearly depending on

$\log P_{\text{O}_2}$ and the slope of the lines is comprised between 0.17 and 0.19, this result being coherent with the presence of the preponderance of V_{O}'' oxygen gaps. For $T < 1200^\circ\text{C}$ and $P_{\text{O}_2} > 10^{-2}$ atm, can observe a deviation from the linearity of the representations $\log \sigma = f(\log P_{\text{O}_2})$, this effect being attributed to impurities preponderant influence.

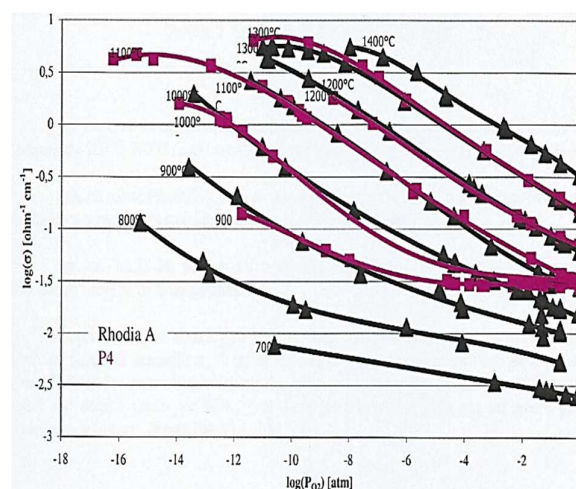


Fig.13. Comparison between electrical conductivities varying with the partial pressure of oxygen, and with temperature (700°C - 1400°C), for the samples A (ceria non-doped) and D (opaline micronized)

Comparison between electrical conductivities varying with the partial pressure of oxygen, and with temperature (700°C - 1400°C), for the samples A (ceria non-doped) and P4 (ceria opaline micronized) is remarked in figure 13. The ceria opaline micronized presents superior transport properties that ceria non-doped.

4. CONCLUSIONS

This study allowed us to notice that ceria doped with Gd (10 mol% Gd_2O_3) is an ionic conductor, because gadolinium behaves like a donor element - defaults Gd_{Ce}' , knowing that ceria non-doped is an n-type semiconductor and that most defects are oxygen vacancies.

In the case of sample P2, grace of the uniaxial isostatic pressure of 25 MPa used for compacting, it can remark a fine granulometry and a good density of the sintering compact sample, around 95%.

The results obtained with undoped cerine have shown us the preponderant influence of grain

boundaries on electrical conductivity, when the temperature decreases, which results in an increase in conductivity.

The presence of gadolinium limits grain enlargement. The thermic treatment realized in Argon C atmosphere conducted at a porosity amelioration, near to 96% density, as in the case of sample B.

The results obtained on the samples doped with gadolinium, show that the electrical conductivity of the grains is not influenced by the method of obtaining the samples and that the electrical conductivity of the grain boundaries is higher when the density samples increase. On the other hand, the activation energy is not influenced by the sintering conditions ($E_a=0.104\text{eV}$).

5. REFERENCES

- [1] Baiutti, F., Portals, J.B., Anelli, S., Torruella, P., Lopez-Haro, M., Calvino, J., Estrade, S., Torell, M., Peiro, F., Tarancon, A., Tailoring the Transport Properties of Mesoporous Doped Cerium Oxide for Energy Applications. *J Phys Chem C*, 125(30), 16451-16463, 2021.
- [2] Yuan, X., Wu, X., Wu, Y., Van Ree, T., Metal oxides for emission control, *Metal Oxides in Energy Technologies*, Metal Oxides, pp.391-414, 2018. <https://doi.org/10.1016/B978-0-12-811167-3.00015-8>.
- [3] Mourya, A., Mazumdar, B., Sinha, S.K., Application of CeO_2 -MWCNTs nanocomposite for heavy metal ion detection in aqueous solutions by electrochemical technique, *Cleaner Materials*, 2, 100021, 2021, <https://doi.org/10.1016/j.clema.2021.100021>
- [4] Chiang, Y.M., Lavik, E.B., Kosacki, I., Tuller, H.L., Ying, J.Y., Defect and transport properties of nanocrystalline CeO_{2-x} , *Appl Phys Lett*, 69, 185-187, 1996, <https://doi.org/10.1063/1.117366>
- [5] Leal, J.J.P., Barrio, R.A., Modelling the structure of disordered cerium oxide thin films, *Physica A: Statistical mechanics and its applications*, 483, 259-265, 2017
- [6] Ramesh, S., Transport properties of SM doped CeO_2 ceramics, *Processing and Application of Ceramics*, 15 (4), 366-373, 2021.
- [7] Schwartz, K.B., Duba A.G., Electrical transport properties of scandium gadolinium garnet, *Journal of Physics and chemistry of solids*, 46(8), 957-962, 1985, [https://doi.org/10.1016/0022-3697\(85\)90099-X](https://doi.org/10.1016/0022-3697(85)90099-X)
- [8] Tuller, H.L., Nowick, A.S., The temperature and oxygen pressure dependence of the ionic transference number of nonstoichiometric CeO_{2-x} *J. Electrochem. Soc.* 122, 255 (1975). <http://doi.org/10.1149/1.2134341>

Proprietățile de transport ale oxidului de ceriu dopat în gadolinium utilizat pentru fabricarea bateriilor electrice

În practica, în inginerie, celulele de combustie cu electroliți solizi sunt o alternativă din ce în ce mai utilizată pentru generarea de energie clean, dar temperaturile ridicate de funcționare necesare (800°C - 1000°C) pot fi un obstacol în calea comercializării acestora. Deci, există cercetări asupra materialelor care pot fi folosite la temperaturi mai scăzute. Pentru a reduce pierderile potențiale, este necesar să se găsească un electrolit cu o conductivitate ionică bună și o conductivitate electrică scăzută. Oxidul de ceriu dopat este considerat ca fiind un posibil înlocuitor pentru oxidul de zirconiu stabilizat cu oxid de ytriu, care este utilizat frecvent. Este important să se stabilească proprietățile sale electrice înainte de a-l folosi într-o baterie de automobile comercială. Au fost studiate diferite compoziții de oxid de ceriu dopat: 10% și 20% dopaj cu gadolinium. Oxidul de ceriu poate fi dopat cu diferite materiale, cum ar fi: samariu și gadolinium, precum și lantan și ytriu. Acest oxid prezintă, la temperaturi scăzute, o conductivitate mai mare decât zirconia (ZrO_2 - 10 mol % Y_2O_3), ceea ce permite ca temperatura de funcționare a bateriilor electrochimice să fie mai scăzută. În această lucrare a fost prezentată elaborarea policristalelor de oxizi de ceriu dopați cu gadolinium și caracterizarea proprietăților de transport ale acestora.

Diana-Irinel BĂILĂ, Associate Professor, PhD Eng., NUST POLITEHNICA Bucuresti, Department Manufacturing Engineering, baila_d@yahoo.com

Sergiu TONOIU, Professor. PhD Eng., NUST POLITEHNICA Bucuresti, Department Manufacturing Engineering, sergiu.tonoiu@upb.ro